

RELIABILITY ESTIMATION OF A HORIZONTAL AXIS WIND TURBINE USING TAIL MODELING

Nehir Kandemir¹ and Erdem Acar²
TOBB University of Economics and Technology^{1,2}
Ankara, Turkey

ABSTRACT

Reliability of highly safe structural systems can be estimated efficiently by using tail modeling. The main idea of tail modeling is to perform a relatively small number of limit-state function calculations through a sampling scheme, specify a threshold value that defines the tail part, and then fit a probability model to the tail part. The selected threshold value has a significant effect on reliability estimations. This paper aims at drawing some guidelines for proper selection of the threshold value using benchmark mathematical example problems with varying number of random variables, level of nonlinearity and level of safety. Finally, tail modeling is applied to reliability prediction of a horizontal axis wind turbine. It is found that the tail modeling can predict the high reliability of horizontal axis wind turbine efficiently and accurately.

INTRODUCTION

The limit-state function of a structural system is usually evaluated through computationally expensive finite element analyses. The simulation techniques such as Monte Carlo method [Liu, 2001] or its advanced variants (e.g., importance sampling [Melchers, 1989], adaptive importance sampling [Wu, 1994], directional simulation [Nie and Ellingwood, 2000]) require a large number of limit-state evaluations; hence they are not suitable for highly safe structural systems. Alternatively, the analytical methods such as first-/second- order reliability methods (FORM/SORM) are computationally efficient, but their accuracy diminishes as the limit-state function becomes nonlinear. To overcome the drawbacks of these traditional methods, the techniques based on tail modeling have been successfully used for reliability assessment at high reliability levels [Kim et al., 2006; Ramu, 2007; Mourelatos et al., 2009; Acar, 2011].

Reliability estimation using tail modeling is based on approximating the tail of the cumulative distribution function (CDF) of the limit-state function. The main idea is to perform a relatively small number of limit-state function calculations through a sampling scheme (e.g., Monte Carlo sampling, Latin Hypercube sampling), specify a threshold value that defines the tail part, and then fit a probability model (e.g., generalized Pareto distribution) to the tail part. The selected threshold value plays an important role on reliability estimations. Selection of the proper value for threshold has been an active research area and some empirical techniques have been proposed. However, none of these techniques presents a globally accepted solution to threshold selection [Ramu, 2007]. In this paper, the effects of function nonlinearity (measured with the coefficient of determination R^2), and distribution properties (e.g., coefficient of variation, skewness) of random variables on threshold selection are explored.

The paper is organized as follows. Section 2 presents a brief overview of tail modeling. Discussions on selection of the proper threshold value are also provided in Section 2. The benchmark example problems used in this paper are presented in Section 3. Guidelines for threshold selection are presented in Section 4. Tail modeling is then applied to reliability prediction of a horizontal axis wind turbine and the results are given in Section 5. Finally, concluding remarks are listed in Section 6.

¹ Graduate Student in Mechanical Engineering Department: nehir.kandemir@etu.edu.tr

² Associate Professor in Mechanical Engineering Department: acar@etu.edu.tr

OVERVIEW OF TAIL MODELING

Consider the limit-state function $y(\mathbf{x})$, where \mathbf{x} is the vector of random variables. For a large threshold value of y_t (see Figure 1), the region above the threshold (i.e., the tail part) can be approximated by using generalized Pareto distribution (GPD). The GPD approximates the conditional excess distribution of $F_z(z)$, where $z = y - y_t$, through

$$F_z(z) = \begin{cases} 1 - \left(1 + \frac{\xi}{\sigma} z\right)_+^{-\frac{1}{\xi}} & \text{if } \xi \neq 0 \\ 1 - \exp\left(-\frac{z}{\sigma}\right) & \text{if } \xi = 0 \end{cases} \quad (1)$$

where $\langle A \rangle_+ = \max(0, A)$, $z \geq 0$, and $F_z(z)$ is the GPD with shape and scale parameters ξ and σ , respectively.

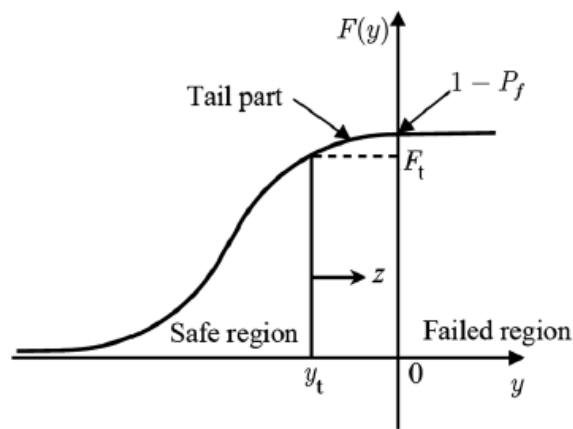


Figure 1: Tail modeling concept

The conditional excess distribution can be related to the cumulative distribution $F(y)$ through

$$F_z(z) = \frac{F(y) - F(y_t)}{1 - F(y_t)} = \frac{F(y) - F_t}{1 - F_t} \quad (2)$$

Then, $F(y)$ above the threshold (i.e., $y \geq y_t$) is expressed in terms of the conditional excess distribution, $F_z(z)$, through

$$F(y) = F_t + (1 - F_t)F_z(y - y_t) \quad (3)$$

Once the cumulative distribution function $F(y)$ is obtained, the probability of failure can be estimated from [Ramu, 2007]

$$P_f = 1 - F(y=0) = (1 - F_t) \left\langle 1 - \frac{\xi}{\sigma} y_t \right\rangle_+^{-\frac{1}{\xi}} \quad (4)$$

Also, the generalized reliability index can be calculated from

$$\beta = \Phi^{-1}(1 - P_f) \quad (5)$$

where Φ is the cumulative distribution function of a standard normal random variable.

As noted earlier, selection of the threshold value has a significant effect on reliability estimations. This will be discussed next in the followings.

Selection of Threshold

There is a tradeoff between bias and variance in threshold selection. If a low threshold is selected, then points belonging to the central part can also contribute to the tail modeling, resulting in bad approximation of the tail. On the other hand, if a high threshold is selected, then the number points used in tail modeling is very small, resulting in large scatter in probability estimation.

Boos [Boos, 1984] recommended the use of $N_t/N=0.2$ for $50 \leq N \leq 500$ and $N_t/N=0.1$ for $500 < N \leq 5000$, where N_t is the number of data that belongs to the tail part, and N is the total number of data. Hasofer [Hasofer, 1996] suggested to use $N_t \approx 1.5\sqrt{N}$. Caers and Maes [Caers and Maes, 1998] proposed that the optimal N_t value can be selected to minimize the mean square error, which can be estimated using bootstrap technique. However, none of these techniques presents a globally accepted solution to threshold selection [Ramu, 2007].

After the threshold value is determined, GPD model parameters (ξ and σ) are estimated. The methods used for determination of GPD model parameters include, maximum likelihood estimation (MLE), method of moments, probability weighted moments, elemental percentile method, the least square regression method. The mostly used and the widely accepted method is the MLE method [Ramu, 2007], so MLE is used in this paper.

EXAMPLE PROBLEMS

To form a guideline, several benchmark example problems with varying number of random variables, nonlinearity and reliability levels and skewness are considered. The details of these example problems are given below.

Branin-Hoo Function

Branin-Hoo function has two random variables x_1 and x_2 following normal distributions. Mean and standard deviation of the random variables are given in Table 1.

Table 1: Mean and standard deviation values of random variables in Branin-Hoo function.

Variable	Mean	Standard Deviation
x_1	2.5	2.5
x_2	7.5	2.5

The limit state function of this problem is given as,

$$Y = y(x_1, x_2) - y_{crit} \quad (6)$$

where the Branin-Hoo function is

$$y(x_1, x_2) = \left(x_2 - \frac{5.1x_1^2}{4\pi^2} + \frac{5x_1}{\pi} - 6 \right)^2 + 10 \left(1 - \frac{1}{8\pi} \right) \cos(x_1) + 10 \quad (7)$$

The ranges of the variables are given as, $x_1 \in [-5, 10]$, and $x_2 \in [0, 15]$. Branin-Hoo function, with the variables at their specified ranges, is illustrated in Fig. 2.

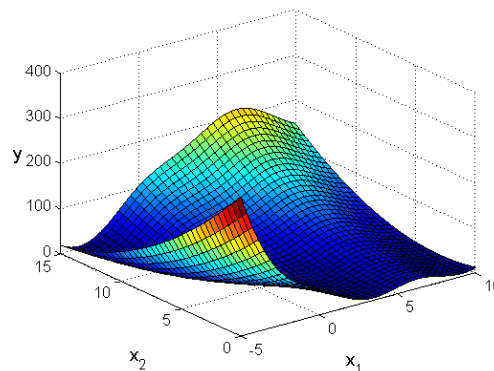


Figure 2: Branin-Hoo function

The value of y_{crit} , computed in Eq. (6) is varied to adjust the reliability level. Various y_{crit} values with corresponding reliability levels are given in Table 2. The reliability indices in Table 2 are computed through Monte Carlo Simulation with a sample size of 100 million

Table 2: Various y_{crit} values with corresponding reliability levels for Branin-Hoo function

y_{crit}	Reliability Index
220	3.30
330	3.83
440	4.15
550	4.44

Camelback Function

Camelback function has two random variables x_1 and x_2 following standard normal distribution. The limit state function of this problem is given as,

$$Y = y(x_1, x_2) - y_{crit} \quad (8)$$

where the Camelback function is

$$y(x_1, x_2) = \left(4 - 2.1x_1^2 + \frac{x_1^4}{3}\right)x_1^2 + x_1x_2 + (-4 + 4x_2^2)x_2^2 \quad (9)$$

Camelback function is illustrated in Fig. 3.

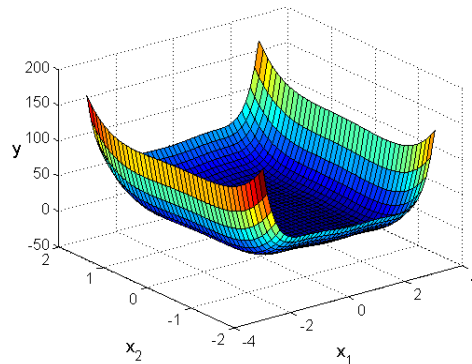


Figure 3: Camelback function

The value of y_{crit} in Eq. (8) is varied to adjust the reliability level. Various y_{crit} values with corresponding reliability levels are given in Table 3.

Table 3: Various y_{crit} values and corresponding reliability indices for Camelback function

y_{crit}	Reliability Index
400	2.95
800	3.52
1400	4.00

Goldstein-Price Function

Goldstein-Price function has two random variables x_1 and x_2 following standard normal distribution. The limit state function of this problem is given as,

$$Y = y(x_1, x_2) - y_{crit} \quad (10)$$

where the Goldstein-Price function is

$$y(x_1, x_2) = [1 + (x_1 + x_2 + 1)^2(19 - 14x_1 + 3x_1^2 - 14x_2 + 6x_1x_2 + 3x_2^2)] \times [30 + (2x_1 - 3x_2)^2(18 - 32x_1 + 12x_1^2 + 48x_2 - 36x_1x_2 + 27x_2^2)] \quad (11)$$

Goldstein-Price function is illustrated in Fig. 4.

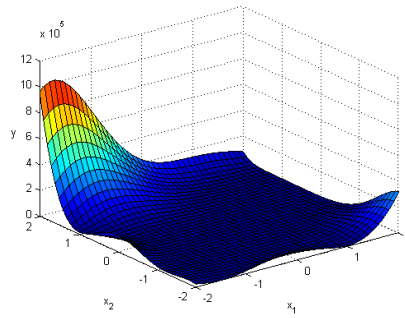


Figure 4: Goldstein-Price function

The value of y_{crit} in Eq. (10) is varied to adjust the reliability level. Various y_{crit} values with corresponding reliability indices are given in Table 4.

Table 4: Various y_{crit} values and corresponding reliability indices for Goldstein-Price function

y_{crit}	Reliability Index
3×10^6	2.74
1×10^7	3.25
3×10^7	3.75
8×10^7	4.25

Sine Function

Goldstein-Price function has two random variables x_1 and x_2 with normal distributions. The mean and standard deviation values for random variables are given in Table 5.

Table 5: Mean and standard deviation values of random variables in Sine function

Variable	Mean	Standard Deviation
x_1	1	3
x_2	1	3

The limit state function of this problem is given as,

$$Y = y(x_1, x_2) - y_{crit} \quad (12)$$

where the Sine function is

$$y(x_1, x_2) = x_1 \sin(x_2) + x_2 \sin(x_1) \quad (13)$$

Sine function is illustrated in Fig. 5

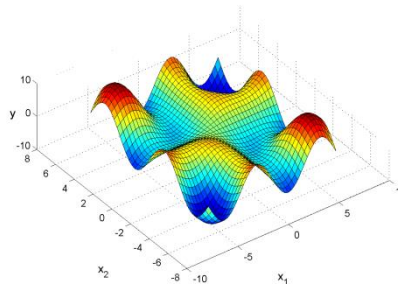


Figure 5: Sine function

The value of y_{crit} in Eq. (12) is varied to adjust the reliability level. Various y_{crit} values with corresponding reliability levels are given in Table 6.

Table 6: Various y_{crit} values with corresponding reliability levels for Sine function

y_{crit}	Reliability Index
9.0	2.53
12.5	3.39
15.5	4.01

Wu's Cantilever Beam Problem

This problem was first introduced by Wu et al. (2001). The cantilever beam illustrated in Fig. 6 has two failure modes: stress failure and excessive displacement. The minimum weight design is sought by varying the width w and thickness t of the beam. The applied loads F_X and F_Y as well as the elastic modulus E and yield strength R are random, all following normal distributions. The random variables' mean and coefficient of variation values as listed in Table 7. The beam width w and thickness t are modeled as deterministic variables.

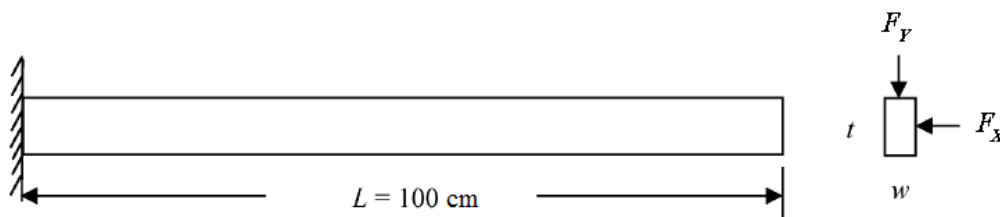


Figure 6: Cantilever beam: geometry and loading

Table 7: Mean and standard deviation values of random variables in Wu's cantilever beam problem.

Variable	Mean	Coefficient of Variation
F_X (N)	500	0.20
F_Y (N)	1000	0.10
E (MPa)	2900	0.05
R (MPa)	400	0.05

The limit-state function corresponding to stress failure mode can be written as

$$y_s = R - \left(\frac{6L}{wt^2} F_Y + \frac{6L}{w^2 t} F_X \right) \quad (14)$$

Similarly, the limit-state function corresponding to displacement failure mode can be written as

$$y_d = D_0 - \frac{4L^3}{Ewt} \sqrt{\left(\frac{F_Y}{t^2} \right)^2 + \left(\frac{F_X}{w^2} \right)^2} \quad (15)$$

where the beam length L is taken as 100 cm and the critical displacement D_0 is set to 2.2535 cm. The geometric properties for minimum weight vary to adjust the reliability level. Various width and height values with corresponding reliability levels are given in Table 8.

Table 8: Various beam designs and corresponding reliability levels for Wu's cantilever beam problem for stress failure mode and displacement failure mode

Width	Height	Stress Reliability Index	Displacement Reliability Index
2.4494	3.8884	3.01	3.01
2.5135	3.9136	3.50	3.65
2.5786	3.9400	4.00	4.34

Tuned Vibration Absorber Problem

The tuned vibration absorber problem is a damped single degree of freedom system with dynamic vibration absorber shown in Fig.7. This example is taken from Kim et al (2006). The original system is externally excited by a harmonic force and the vibration of the system is reduced by the absorber. The amplitude of the vibration depends on the following system parameters:

- $R = \frac{m}{M}$, the mass ratio of the absorber to the original system
- ζ , the damping ratio of the original system
- $\beta_1 = \frac{\omega_{n1}}{\omega}$, the ratio of the natural frequency of the original system to the excitation frequency
- $\beta_2 = \frac{\omega_{n2}}{\omega}$, the ratio of the natural frequency of the absorber to the excitation frequency

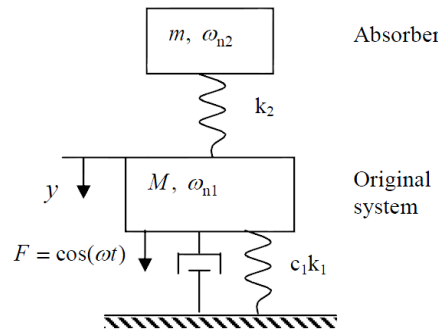


Figure 7: Tuned Vibration Absorber

Tuned vibration absorber problem has two random variables β_1 and β_2 following normal distributions. R and ζ are taken as deterministic variables with the values $R = 0.01$ and $\zeta = 0.01$. Random variables' mean and standard deviation values are given in Table 9.

Table 9: Mean and standard deviation values of random variables in tuned vibration absorber problem

Variable	Mean	Standard Deviation
β_1	1	0.025
β_2	1	0.025

The limit-state function for this problem can be expressed as

$$Y = y(\beta_1, \beta_2) - y_{crit} \quad (16)$$

where $y(\beta_1, \beta_2)$ is the amplitude of the system normalized by the amplitude of the quasi static response of the system, and this normalized amplitude can be calculated from

$$y(\beta_1, \beta_2) = \frac{\left| 1 - \left(\frac{1}{\beta_2} \right)^2 \right|}{\sqrt{\left[1 - R \left(\frac{1}{\beta_1} \right)^2 - \left(\frac{1}{\beta_1} \right)^2 - \left(\frac{1}{\beta_2} \right)^2 + \left(\frac{1}{\beta_1 \beta_2} \right)^2 \right]^2 + 4\zeta^2 \left[\frac{1}{\beta_1} - \frac{1}{\beta_1 \beta_2^2} \right]^2}} \quad (17)$$

The normalized amplitude of the original system is plotted in Fig. 8.

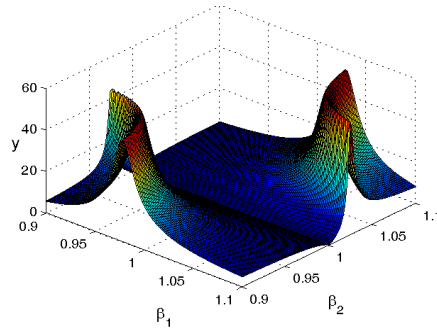


Figure 8: The normalized amplitude of the vibration absorber

The value of y_{crit} in Eq. (16) is varied to adjust the reliability level. Various y_{crit} values with corresponding reliability levels are given in Table 10.

Table 10: Various y_{crit} values with corresponding reliability levels for tuned vibration absorber problem

y_{crit}	Reliability Index
27	2.29
48	3.03
53	3.86

Fortini's Clutch Problem

The overrunning clutch assembly, given in Fig. 9, is known as Fortini's clutch. This example is taken from Lee and Kwak (2006). Fortini's Clutch problem has four random variables x_1 , x_2 , x_3 and x_4 following normal distributions. Random variables' mean and standard deviation values are given in Table 11.

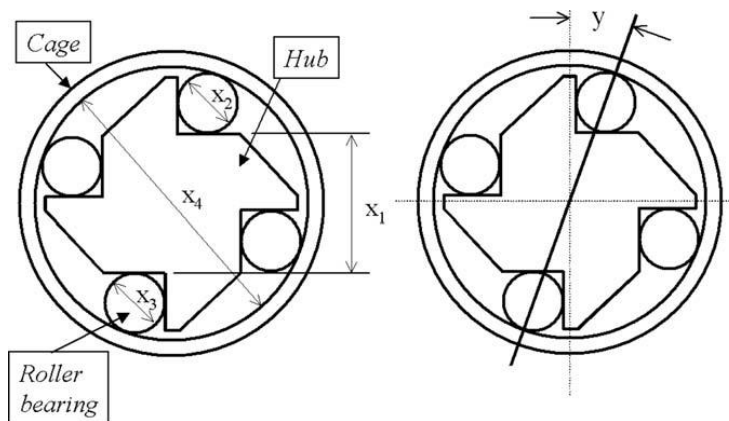


Figure 9: The clutch assembly [Courtesy of Lee and Kwak 2006]

Table 11: Mean and standard deviation values of random variables in Fortini's Clutch problem

Variable	Mean	Standard Deviation
x_1	55.29	0.0793
x_2	22.86	0.0043
x_3	22.86	0.0043
x_4	101.60	0.0793

The limit-state function for this problem can be expressed as

$$Y = y(x_1, x_2, x_3, x_4) - y_{crit} \quad (18)$$

The contact angle y is given in terms of the geometric variables x_1 through x_4 as

$$y(x_1, x_2, x_3, x_4) = \arccos \left[\frac{x_1 + 0.5(x_2 + x_3)}{x_4 - 0.5(x_2 + x_3)} \right] \quad (19)$$

The value of y_{crit} in Eq. (18) is varied to adjust the reliability level. Various y_{crit} values with corresponding reliability levels are given in Table 12.

Table 12: Various y_{crit} values with corresponding reliability levels for Fortini's clutch problem

y_{crit}	Reliability Index
4.5	3.10
4.0	3.55
3.5	3.94

Simply Supported I-beam Design Problem

In this example, a simply-supported I-beam (given in Fig. 10) under a concentrated load as discussed in Huang and Du (2006) is examined. Simply supported I-beam design problem has eight random variables which follow normal distribution. The mean and standard deviation of these variables are summarized in Table 13.

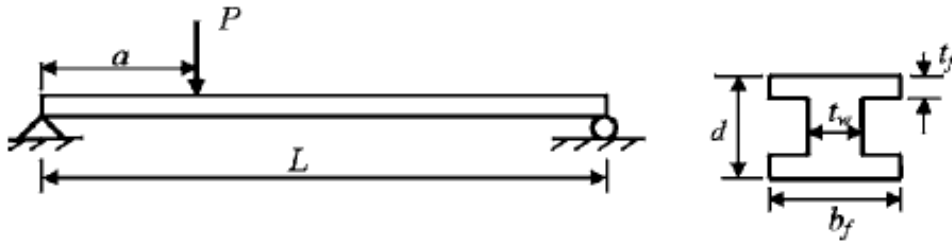


Figure 10: The cross section and loading on the I-beam

Table 13: Mean and standard deviation values of random variables in simply supported I-beam design problem

Variable	Mean	Standard Deviation
P	6070	200
L	120	6
a	72	6
S	170000	4760
d	2.3	1/24
b_f	2.3	1/24
t_w	0.16	1/48
t_f	0.26	1/48

The limit-state function for this problem is formulated as the difference between the strength, S , and load effect in terms of maximum normal stress, σ_{max} due to bending given by

$$Y = \sigma_{max} - S \quad (20)$$

where

$$\sigma_{max} = \frac{Pa(L-a)d}{2LI}; \quad I = \frac{b_f d^3 - (b_f - t_w)(d - 2t_f)^3}{12} \quad (21)$$

The value of S in Eq. (20) is varied to adjust the reliability level. Various S values with corresponding reliability levels are given in Table 14.

Table 14: Various S values with corresponding reliability levels for Simply Supported I-beam Design problem

S	Reliability Index
30,000	2.76
40,000	3.26
50,000	3.73

GUIDELINES FOR THRESHOLD SELECTION

To develop a guideline, tail modeling is applied to all example problems. For all problems, $N=500$ samples of each random variable are generated from the given distribution types and then limit state functions are calculated and sorted. Threshold value is changed from 0.80 to 0.99 by 0.01 at each step and the tail portion is defined. Generalized Pareto distribution (GPD) is fitted to the tail portion, scale and shape parameters are estimated and corresponding reliability index values are calculated. The overall procedure is repeated for 1000 times and root mean square error (RMSE) for reliability index estimations is calculated. RMSE is chosen because it combines the effect of both bias and variance. Finally the threshold value for minimum RMSE is determined. Figure 11 shows the variation of bias, variance and RMSE for Branin-Hoo (when $y_{crit}=220$) and Camelback (when $y_{crit}=400$) example problems. For Branin-Hoo problem, the threshold value for minimum bias is $F_t=0.85$, the threshold value for minimum variance is $F_t=0.99$, and the threshold value for minimum RMSE is also $F_t=0.99$ as seen from Fig. 11(a). It is shown in Fig. 11(b) that the critical threshold values for Camelback problem are different from Branin-Hoo problem so that the threshold value for minimum bias is $F_t=0.99$, the threshold value for minimum variance is $F_t=0.80$, and the threshold value for minimum RMSE is $F_t=0.91$.

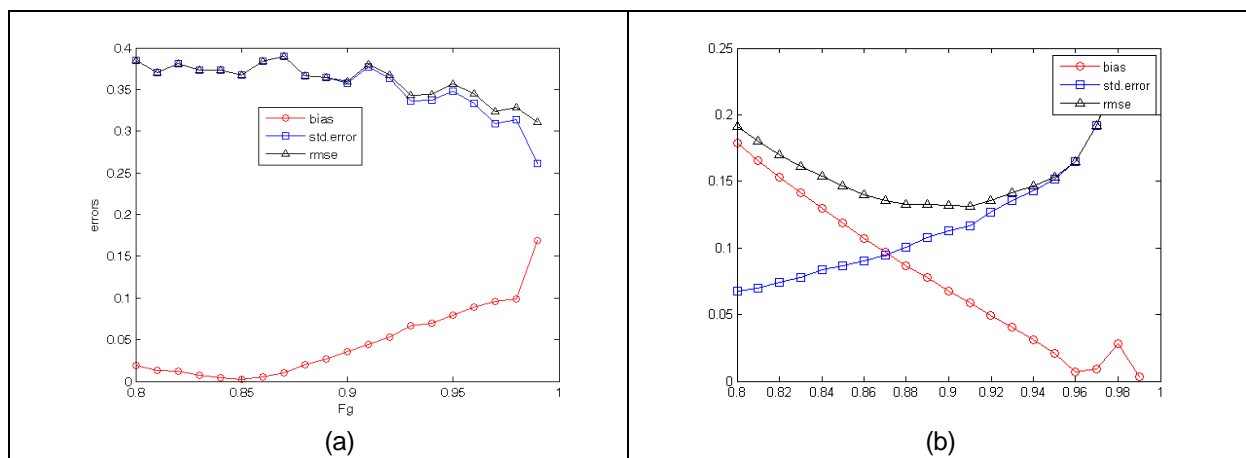


Figure 11: Variation of bias, variance and RMSE for Branin-Hoo (when $y_{crit}=220$) and Camelback (when $y_{crit}=400$) problems

For all example problems, coefficient of determination (R^2), coefficient of variation, and skewness values are also calculated and variation of these parameters with the threshold for minimum RMSE are obtained. Figures 12 through 14 show that the dependence of the threshold selection on the number of variables, R^2 , the coefficient of variation, and skewness is very complex and far from being linear. Based on the results obtained from all example problems, the use of $F_t=0.90$ is found to be a proper threshold value.

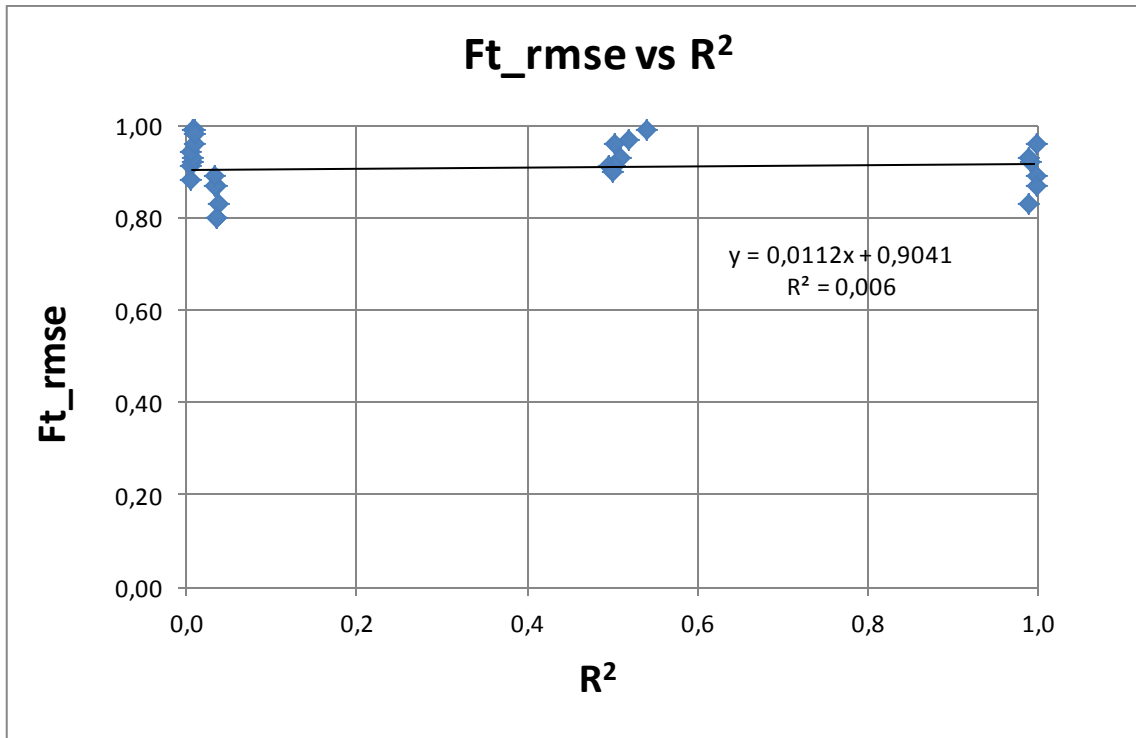


Figure 12: Relationship between the threshold value and R²

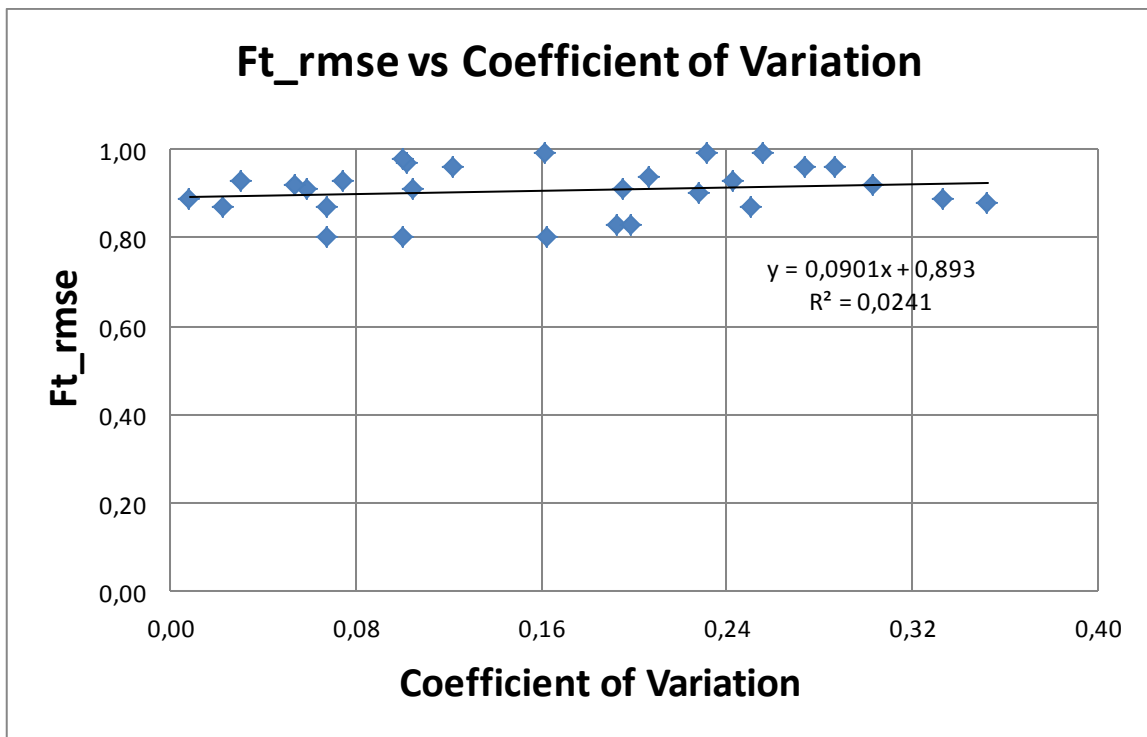


Figure 13: Relationship between the threshold value and coefficient of variation

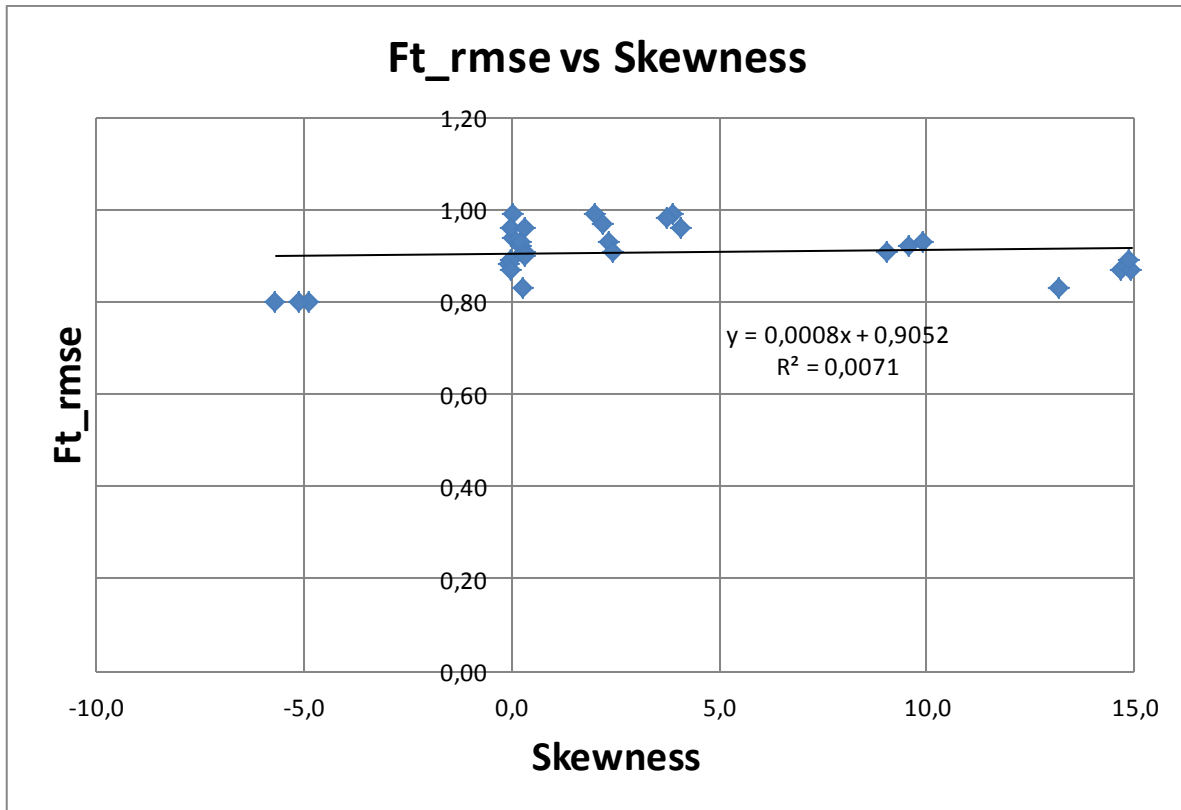


Figure 14: Relationship between the threshold value and skewness

APPLICATION TO RELIABILITY PREDICTION OF A HORIZONTAL AXIS WIND TURBINE

Wind turbines are used to convert wind power to electrical energy. Based on their rotation types, wind turbines can be divided into two categories as vertical axis wind turbines (VAWT) and horizontal axis wind turbines (HAWT). Today, HAWTs are used for most of the electricity production. Capacity of a wind turbine changes due to its diameter. As turbine diameter increases, the capacity of the wind turbine also increases. Wind turbine development over years by means of both diameter size and capacity is given in Figure 15.

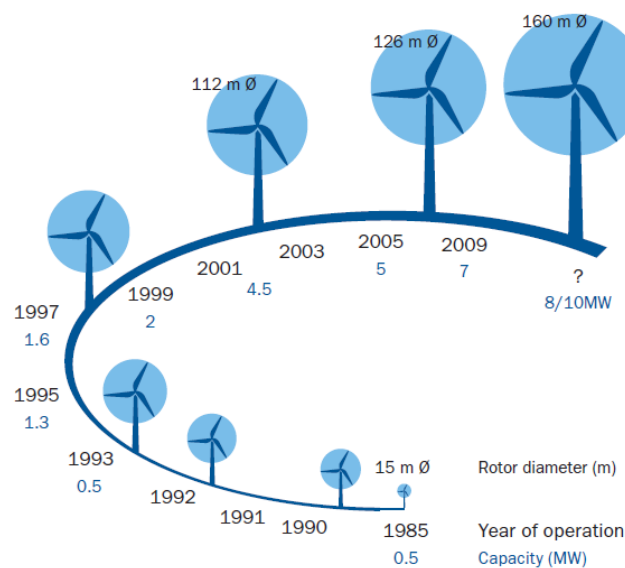
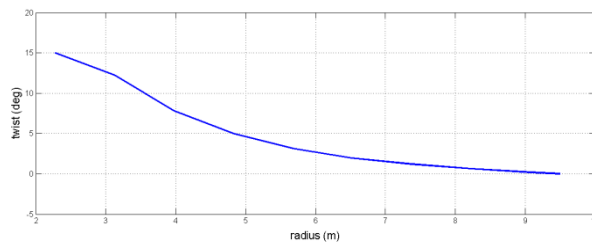


Figure 15: Wind turbine development [Courtesy of European Wind Energy Association, 2010]

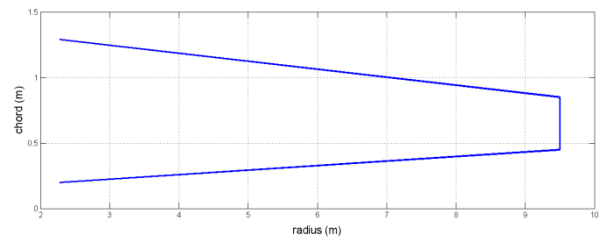
In this section, reliability prediction of Risoe wind turbine is considered. Risoe wind turbine is a 100 kW HAWT developed by Denmark Technical University National Laboratory for Sustainable Energy to be used for field testing purposes. The reason for choosing this particular wind turbine is that there exist detailed accessible information on turbine geometry and other characteristics in many sources including the U.S. National Renewable Energy Laboratory (NREL). Table 15 provides the geometrical characteristics of Risoe wind turbine, taken from Ceyhan et al., 2009. Risoe wind turbine blades are twisted and tapered (see Figure 16), and use NACA 63-4xx series airfoils.

Table 15: General characteristics of Risoe wind turbine [Ceyhan et al., 2009]

Number of Blades	3
Turbine diameter	19 m
Rotational Speed	47.5 rpm
Cut-in wind speed	4 m/s
Control type	Stall
Rated power	100 kW
Root extension	2.3 m
Blade set angle	1.8 degree
Maximum Twist	15 degree
Root Chord	1.09 m
Tip Chord	0.45 m
Airfoil	NACA 63-4xx series



(a) twist variation



(b) taper variation

Figure 16: Twist and taper variation of Risoe wind turbine blades over the chord

In this application problem, the aerodynamic performance of Risoe WT blades is considered. The aerodynamic performance of the WT is measured by its ability to provide at least 100 kW power when the wind speed is at the maximum power wind speed of 13.5 m/s. The power generated by the WT is evaluated using WT_Perf software (a free software developed by NREL) that uses the blade element momentum theory.

Blade element momentum theory (BEMT) is one of the oldest and most commonly used methods for evaluating the aerodynamic performance of wind turbines. BEMT is a combination of blade element theory and momentum theory [Burton et al., 2001]. Even though the theory is based on many assumptions, it still provides satisfactory results at low wind speed values [Snel 2003, Ceyhan et al. 2009]. In this theory, the flow is assumed to be continuous, homogeneous, steady-state, incompressible, axisymmetric and the turbulence effects are ignored.

In blade element theory, the blades are divided into a large number of elements that operate as two-dimensional hydrofoils with and the aerodynamic behaviors the elements are assumed to be independent of one another. The aerodynamic forces on the elements are calculated on the basis of local flow conditions. Total force and moment on the turbine are calculated by integrating the element forces along the wing span.

In momentum theory (actuator disc theory), the work done by the air flow on the blade elements is the main cause of loss of pressure or momentum. The momentum losses in axial and tangential directions can be calculated using the induced velocities in the axial and tangential directions.

The geometry as well as the lift and drag characteristics of the rotor determine the capability of rotor to extract power from a moving fluid. Blending these two theories, BEMT is used to compute the capability of rotor to extract power from a moving fluid. Detailed information on BEMT can be found in Burton et al., 2001.

The comparison of the WT_Perf predictions and the Risoe wind turbine test data is provided in Figure 17. It is seen that the performance of WT_Perf is very good at low velocities as expected. It is also observed that the performance of WT_Perf at the maximum power wind speed of 13.5 m/s is satisfactory.

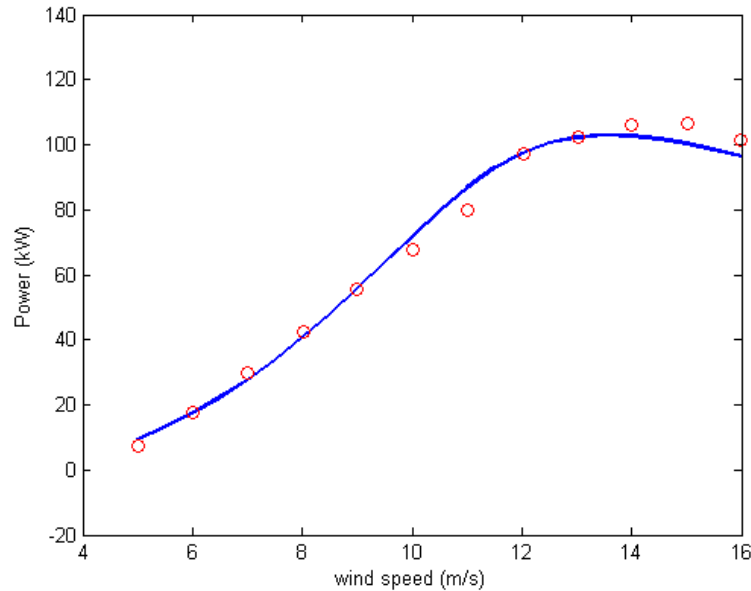


Figure 17: Comparison of the WT_Perf predictions and the Risoe wind turbine test data

The random variables for Risoe wind turbine problem are listed in Table 16. All random variables are assumed to follow normal distribution, with the mean and standard deviation values given in Table 16.

Table 16: Random variables for Risoe wind turbine problem

Random variable	Mean	Standard deviation
Turbine radius	9.5 m	0.01 m
Rotational Speed	47.5 rpm	0.03 rpm
Cut-in wind speed	4 m/s	0.1 m/s
Root extension	2.3 m	0.01 m
Blade set angle	1.8 degree	0.05 degree
Maximum Twist	15 degree	0.5 degree
Root Chord	1.09 m	0.01 m
Tip Chord	0.45 m	0.01 m

The reliability of the Risoe WT is first evaluated through Monte Carlo Simulation (MCS) with $N=1,000,000$ samples to provide a baseline for comparison for tail modeling predictions. A histogram is plotted for the calculated power values to observe its distribution type. The histogram of power for $N=1,000,000$ is given in Figure 18. As can be seen from Figure 18, the distribution type of the calculated power values is close to normal distribution. The calculated skewness and kurtosis values of power also support resemblance to normal distribution. Mean and standard deviation values of the calculated power values along with its skewness and kurtosis values are summarized at Table 17.

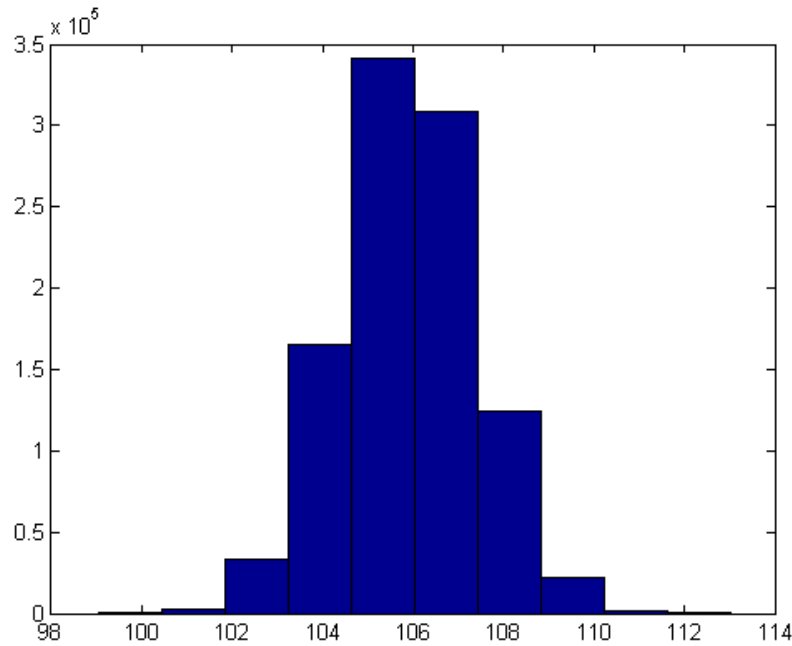
Figure 18: Histogram of power values for $N=1,000,000$

Table 17: Mean, standard deviation, skewness and kurtosis values of the calculated power values

Mean [kW]	105.8796
Standard Deviation [kW]	1.4808
Skewness	0.0273
Kurtosis	2.9853

From the MCS results, it is observed that 30 out of 1,000,000 samples fail, therefore the failure probability can be estimated as $P_f=3 \times 10^{-5}$. The corresponding reliability index for this value of failure probability is $\beta=4.0128$ (see Table 18). The confidence level due to limited MCS sampling is also given in Table 18.

Tail modeling is finally applied to the reliability prediction of Risoe wind turbine. $N=500$ samples of each random variable are generated from the normal distribution and then limit state functions are calculated and sorted. The limit state function is calculated as;

$$y = -p + p_{crit} \quad (22)$$

where y denotes limit state function, p is the power generated by WT and p_{crit} is 100 kW. In order to define the tail portion, threshold value of $F_t=0.90$ is used. Generalized Pareto distribution is fitted to the tail portion, scale and shape parameters are found and the corresponding reliability index values are calculated. The overall procedure is repeated for a 1000 times to reduce the effect of random sampling. Tail modeling predictions of reliability index are compared to MCS prediction in Table 18. It is found that the tail modeling method can predict this high reliability of the WT efficiently and accurately.

Table 18: The reliability index values for Monte Carlo Simulation and Tail Modeling

	N	β
Monte Carlo Simulation	1,000,000	4.0128 (3.97, 4.06)*
Tail Modeling	500	4.1352

*The confidence level due to limited MCS sampling

CONCLUDING REMARKS

Reliability estimation using tail modeling is based on approximating the tail of the limit-state function's cumulative distribution function. For a specified threshold value that defines the tail part, generalized Pareto distribution (GPD) is fitted to the tail part, scale and shape parameters are found and corresponding reliability index values are calculated. In this study, tail modeling is applied to benchmark mathematical example problems of varying number of random variables, nonlinearity level, coefficient variation and skewness. The threshold value for minimum RMSE is computed for all these problems. It is seen that the dependence of the proper threshold value on the number of variables, the coefficient of variation, R^2 and skewness is very complex and far from being linear. The proper threshold value is determined as $F_t=0.90$.

Tail modeling is applied to reliability prediction of a horizontal axis wind turbine. The reliability predictions through tail modeling are compared to Monte Carlo simulation predictions to validate the tail modeling predictions. The reliability index prediction obtained from tail modeling is different from MCS prediction by 3%. This indicates that the tail modeling can accurately predict high reliability of HAWT.

References

- Acar, E., 2011, "Guided Tail Modeling for Efficient and Accurate Reliability Estimation of Highly Safe Mechanical Systems," *Proceedings of the Institution of Mechanical Engineers Part C: Journal of Mechanical Engineering Science*, Vol. 225, No. 5, pp. 1237-1251.
- Boos, D., 1984, "Using Extreme Value Theory to Estimate Large Percentiles," *Technometrics*, 26 (1) 33-39.
- Burton T., Sharpe D., Jenkins N., Bossanyi E., "Wind Energy Handbook," John Wiley and Sons, 2001.
- Caers, J., and Maes, M., 1998, "Identifying Tails, Bounds, and End-Points of Random Variables," *Structural Safety*, Vol. 20, pp. 1-23.
- Ceyhan, O., Ortakaya, Y., Korkem, B., Sezer-Uzol, N. and Tuncer, I.H., 2009, "Optimization of Horizontal Axis Wind Turbines by Using BEM Theory and Genetic Algorithm," *5th Ankara International Aerospace Conference*, Ankara, AIAC-2009-044.
- European Wind Energy Association (EWEA), Wind Energy Factsheets 2010, http://www.ewea.org/fileadmin/ewea_documents/documents/publications/factsheets/Factsheets.pdf, as accurate of July 2013.
- Hasofer, A., 1996, "Non-Parametric Estimation of Failure Probabilities," *Mathematical Models for Structural Reliability*, Eds. F. Casciati, and B. Roberts, CRC Press, Boca Raton, FL, 195-226.
- Kim, N.H., Ramu, P., and Queipo, N.V., 2006, "Tail Modeling in Reliability-Based Design Optimization for Highly Safe Structural Systems," *47th AIAA/ASME/ASCE/AHS/ASC Structures, Structural Dynamics, and Materials Conference*, Newport, RI, AIAA 2006-1825.
- Liu, J.S., 2001, "Monte Carlo Strategies in Scientific Computing," Springer-Verlag, New York.
- Melchers, R.E., 1989, "Importance Sampling in Structural Systems," *Structural Safety*, Vol. 6, pp. 3-10.
- Mourelatos, Z.P., Song, J., and Nikolaidis, E., 2009, "Reliability Estimation of Large-Scale Dynamic Systems by using Re-analysis and Tail Modeling," *SAE World Congress & Exhibition*, Detroit, MI, April 2009, Paper No. 2009-01-0200.
- Nie, J., and Ellingwood, B.R., 2000, "Directional Methods for Structural Reliability Analysis," *Structural Safety*, Vol. 22, pp. 233-249.
- Ramu, P., 2007, "Multiple Tail Models Including Inverse Measures for Structural Design Under Uncertainties," PhD thesis, University of Florida, Gainesville, FL.
- Snel H., "Review of Aerodynamics for Wind Turbines," *Wind Energy*, Vol. 6, 2003, pp 203-211.
- Wu, Y.T., 1994, "Computational Methods for Efficient Structural Reliability and Reliability Sensitivity Analysis," *AIAA Journal*, Vol. 32, No. 8, pp. 1717-1723.